

# Polyacrylamide gel synthesis and sintering of $\text{Mg}_2\text{SiO}_4\text{:Eu}^{3+}$ nanopowder

S.A. Hassanzadeh-Tabrizi<sup>a,\*</sup>, E. Taheri-Nassaj<sup>b</sup>

<sup>a</sup>Department of Materials Engineering, Najafabad Branch, Islamic Azad University, Isfahan, Iran

<sup>b</sup>Department of Materials Science and Engineering, Tarbiat Modares University, P.O. Box 14115-143, Tehran, Iran

Received 9 January 2013; received in revised form 13 January 2013; accepted 16 January 2013

Available online 1 February 2013

## Abstract

A  $\text{Mg}_2\text{SiO}_4\text{:Eu}^{3+}$  nanopowder was synthesized by a polyacrylamide gel method. In this route, the gelation of the solution is achieved by the formation of a polymer network which provides a structural framework for the growth of particles. The densification of the powders was also studied. An amorphous nanopowder was synthesized and crystallized to  $\text{Mg}_2\text{SiO}_4$  after heat-treatment via a solid-state reaction at a relatively low temperature of about 700 °C. The powders prepared by the polyacrylamide gel method showed better sinterability than the powders synthesized by the conventional sol–gel method. The relative density of the sample was 97% at 1500 °C. © 2013 Elsevier Ltd and Techna Group S.r.l. All rights reserved.

**Keywords:** A. Sintering;  $\text{Mg}_2\text{SiO}_4$ ; Chemical synthesis; Nanostructures

## 1. Introduction

Forsterite ( $\text{Mg}_2\text{SiO}_4$ ) is a member of the olivine family and has orthorhombic crystalline structure, which has high surface area, low thermal expansion, good chemical stability and excellent insulation properties even at high temperatures. In addition it has low electrical conductivity that makes it an ideal substrate material in electronics [1–3].

Forsterite doped with a small amount of impurities is used as optical host materials. For instance, chromium-doped forsterite has been recently found to be an excellent laser material in the tunable near-infrared range of 1.1–1.3  $\mu\text{m}$  [4]. Among the rare earth ions, red-emitting trivalent europium ( $\text{Eu}^{3+}$ ) is recognized as an efficient red luminescent phosphors which are used in color television displays and mercury free lamps [5–7]. Owing to such application potential of  $\text{Mg}_2\text{SiO}_4$ , a lot of efforts have been made to try to synthesize forsterite ceramics. Generally,  $\text{Mg}_2\text{SiO}_4$  is prepared at high temperatures for an extended time period via a solid-state reaction process. Such traditional process normally leads to powders with large grain sizes. Moreover, the final product is

not homogenous and has some undesirable  $\text{MgSiO}_3$  phase [8–10]. For correcting these drawbacks of the solid-state reaction process, many wet chemical methods have been developed and successfully used for powder processing in recent years [10–12]. The polyacrylamide gel process was a fast, cheap, reproducible and easily scaled up chemical route for obtaining fine powders [13,14]. During the synthesis process, because the metal ions are completely dissolved in polymeric resin, the polyacrylamide gel synthesis provides a molecular level mixing of elements.

The object of the present research is synthesis of  $\text{Mg}_2\text{SiO}_4\text{:Eu}^{3+}$  nanopowder from magnesium nitrate, Tetra ethyl ortho-silicate and europium nitrate at low temperatures using a polyacrylamide gel method. The structure, particle size and densification of the powders have been investigated. In addition the synthesized powders were compared with the powders prepared by a conventional sol–gel method.

## 2. Experimental procedure

The  $\text{Mg}_2\text{SiO}_4$  nanopowders with 1 mol% concentration of  $\text{Eu}^{3+}$  ions were prepared using polyacrylamide gel method. Magnesium nitrate hexahydrate ( $\text{Mg}(\text{NO}_3)_2 \cdot 6\text{H}_2\text{O}$ , Merck), tetra ethyl ortho-silicate (TEOS, Merck) and europium

\*Corresponding author. Tel.: +98 331 2291111; fax: +98 331 2291016.

E-mail addresses: [hassanzadeh@pmt.iaun.ac.ir](mailto:hassanzadeh@pmt.iaun.ac.ir),  
[tabrizi1980@gmail.com](mailto:tabrizi1980@gmail.com) (S.A. Hassanzadeh-Tabrizi).

nitrate ( $\text{Eu}(\text{NO}_3)_3$ , Merck) were used as starting magnesium, silicon and europium precursors. The TEOS was dissolved in 1 M  $\text{HNO}_3$ . To this solution  $\text{Mg}(\text{NO}_3)_2 \cdot 6\text{H}_2\text{O}$  and  $\text{Eu}(\text{NO}_3)_3$  were added and stirred for 2 h at room temperature. The pH of the solution was measured to be about 4. Acrylamide (AM) and  $N,N'$ -methylene bis acrylamide (MBAM) monomers as polymerization agents were added in the prepared solution. The free-radical crosslinking copolymerization of AM and MBAM was initiated by adding  $N,N,N',N'$ -tetramethyl ethylene diamide (TEMED) and ammonium persulfate (APS) to the mixture. In this state, a transparent gel was rapidly obtained. For comparison, one specimen was prepared without polymeric agents (conventional sol–gel method). For preparing of this sample, the metal salts were dissolved in deionized water. HCl was added to the solution and the pH value of the solution was adjusted at 2. This precursor solution was continuously stirred at  $100^\circ\text{C}$  and then placed in an oven at  $60^\circ\text{C}$  for 3 h. The viscosity of the solution gradually increased and finally a rigid gel obtained.

The gels were dried at  $80^\circ\text{C}$  for 48 h and calcined at  $600^\circ\text{C}$ . In order to reduce the amount of agglomerates, the calcined nanopowder was wet-planetary milled for 1 h. The powders were pressed into compacts, using a uniaxial press at the pressure of 300 MPa. The compacts were then sintered in a tube furnace under oxygen atmosphere at various temperatures for 3 h with a heating rate of  $6^\circ\text{C}/\text{min}$ .

The crystalline structure of the powder was determined by X-ray diffraction using a Philips X-pert model with  $\text{Cu K}\alpha$  radiation. Differential thermal analyses (DTA) and thermogravimetric (TG) were used with STA equipment (PL Thermal Sciences STA 1500, U.K.). The microstructure of the powder was observed by transmission electron microscopy (TEM; CM200-Phillips, Netherlands). The chemical groups of the powders were analyzed with Fourier transformation infrared spectroscopy (FTIR, Nicolet Nexus 6700).  $\text{N}_2$  adsorption–desorption isotherms were determined in a surface analyzer equipment (BEL Japan Inc., Osaka, Japan) at 77 K. BET surface area and BJH analyses were used to determine the total specific surface area and the pore size distribution. The densities of the sintered specimens were measured by the Archimedes method.

### 3. Results and discussion

Fig. 1 shows X-ray diffraction patterns of as-received and calcined powders synthesized by the polyacrylamide gel method at different temperatures. As can be seen all the as-produced samples are completely amorphous. Forsterite has begun to form around  $700^\circ\text{C}$ . The pattern was compared with JCPDS file No. 34-0189. With increasing temperature from 700 to  $800^\circ\text{C}$  a sudden increase in the intensity of forsterite reflections accompanied by sharpening of them occurred. No peaks characterizing any other phase were detected. By increasing the heat-treatment temperature, the broadening of the peaks decreases which shows the growing  $\text{Mg}_2\text{SiO}_4$  nanocrystallites.

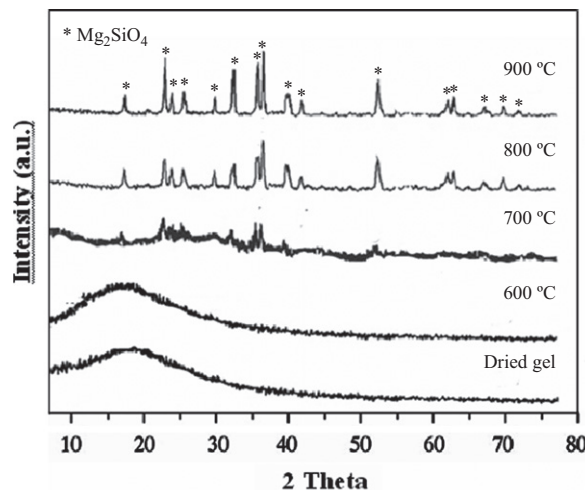


Fig. 1. The XRD patterns of samples heat treated at various temperatures for 3 h.

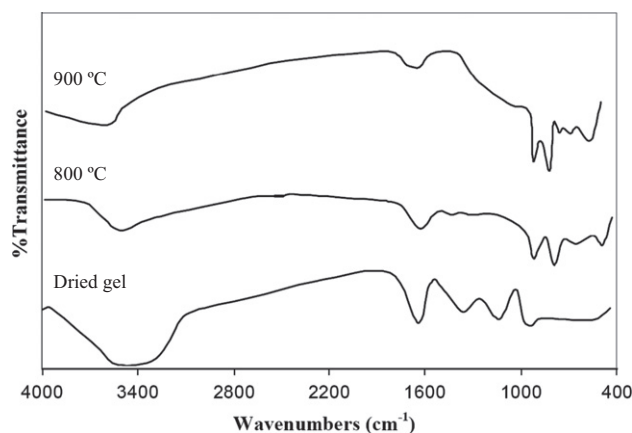


Fig. 2. IR spectra of powders heat treated at various temperatures. Fig. 4 IR spectra of powders heat treated at various temperatures.

Fig. 2 represents the Fourier transformation infrared spectroscopy (FTIR) spectra of the powders heat-treated at various temperatures for 3 h. The absorption broad peak at  $3000\text{--}3600\text{ cm}^{-1}$  [15] and absorption peak at around  $1640\text{ cm}^{-1}$  [15] correspond to the  $\nu(\text{O}\text{--}\text{H})$  and  $\delta(\text{O}\text{--}\text{H})$  vibration of water, respectively. Additionally, the frequencies in the ranges of  $1200\text{--}1400\text{ cm}^{-1}$  are assigned to C–H, C–O stretching arising from organic residuals [16]. The peaks between  $1000$  and  $1100\text{ cm}^{-1}$  is related to Si–O–Si bands. The decrease in intensities of mentioned bands and disappearance of them at  $900^\circ\text{C}$  is accompanied with the shift of Si–O–Si related peaks to lower wave numbers because of strengthening of Si–O bands in the  $\text{SiO}_4$  tetrahedron that prove the formation of forsterite as it is shown in XRD of this sample. In calcined powders at  $900^\circ\text{C}$ , the bands related to the characteristic peaks of forsterite appear in the range of  $830\text{--}1000\text{ cm}^{-1}$  and  $500\text{--}620\text{ cm}^{-1}$  for  $\text{SiO}_4$  and at  $475\text{ cm}^{-1}$  for modes of octahedral  $\text{MgO}_6$  [17]. However, weaker bands at  $3000\text{--}3500$  and  $1640\text{ cm}^{-1}$  could still be observed, which are probably due to the fact that the spectra are not recorded

in situ and the absorption of  $\text{H}_2\text{O}$ , from the ambient atmosphere has occurred.

Fig. 3 shows the DTA and TG plots of the powders prepared via the conventional sol–gel and polyacrylamide gel methods. The DTA curve of the powders prepared by the conventional sol–gel method shows an endothermic peak at  $196^\circ\text{C}$  which is attributed to evaporation of absorbed water and dehydration of the dried gel. Corresponding weight loss of 30% appears in the TG curve. The DTA curve of the powders synthesized by the polyacrylamide gel method shows two exothermic peaks at  $240$  and  $425^\circ\text{C}$ . The first exothermic peak has a rather broad nature covering a temperature range of  $156$ – $320^\circ\text{C}$ . In contrast, the second exothermic peak is quite sharp. The TG curve, on the other hand, shows total weight loss of about 80%, which takes place in three stages. In the first stage ( $80$ – $215^\circ\text{C}$ ), the weight loss is about 19%. The second stage of weight loss occurring in the temperature range ( $215$ – $419^\circ\text{C}$ ) is about 33%. The third stage of weight loss (28%) is observed between  $419$  and  $560^\circ\text{C}$ . The first exothermic reaction with a large weight loss is likely attributed to decomposition of side-chain of polyacrylamide [18]. The second exothermic weight loss at  $425^\circ\text{C}$  is caused by decomposition of polyacrylamide's backbone and other residues [18]. No further weight loss is detected above  $560^\circ\text{C}$ , indicating that the organic phase has been completely burned off. As can be seen the weight loss of powders prepared by the polyacrylamide gel method is much more than that in the powders

prepared via the conventional sol–gel. This is attributed to the existence of organic component in the powders produced by the polymeric route.

The nitrogen adsorption–desorption isotherm at  $77\text{ K}$  and the BJH pore size distribution of  $\text{Mg}_2\text{SiO}_4\cdot\text{Eu}^{3+}$  powders prepared by the polyacrylamide gel method and calcined at  $900^\circ\text{C}$  are shown in Fig. 4. It can be seen that the powder exhibits the classical shape of a type IV isotherm according to the IUPAC classification, typical for mesoporous solids [19]. The existence of the hysteresis loop in the isotherm is due to the capillary condensation of nitrogen gas in the mesopores. The similar hysteresis loop was also observed in the powders synthesized via the conventional sol–gel method (not shown here). The surface area and the mean pore diameter of the powders calcined at  $900^\circ\text{C}$  are shown in Table 1. It is clear that the powders prepared by the polyacrylamide gel method shows higher surface area than that powders prepared by the conventional sol–gel method. The BET surface areas of the particles can be related to the primary particle size by the following equation [20,21]:

$$S = \frac{6000}{D\rho} \quad (1)$$

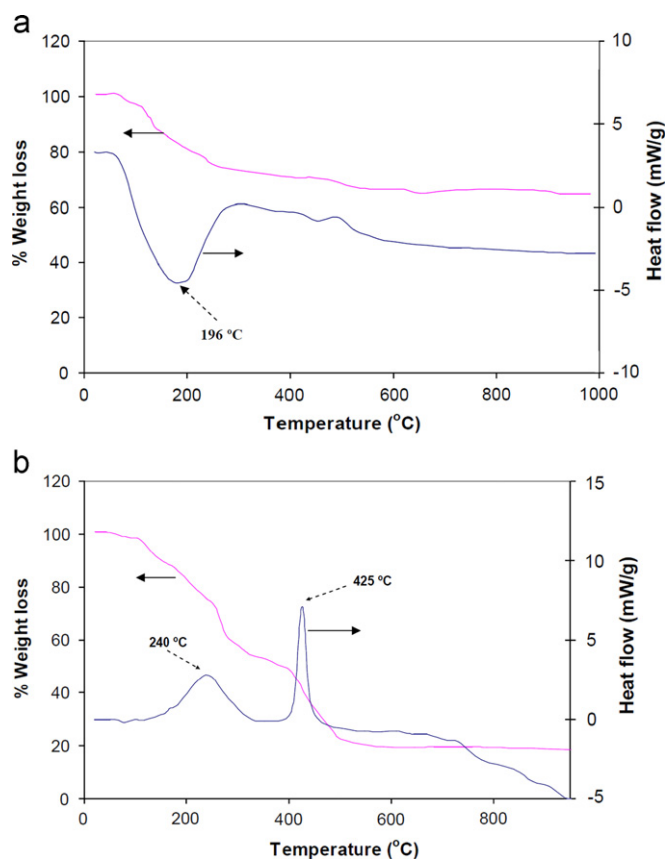


Fig. 3. DTA and TG curves of the gel prepared by (a) the conventional sol–gel and (b) polyacrylamide gel methods.

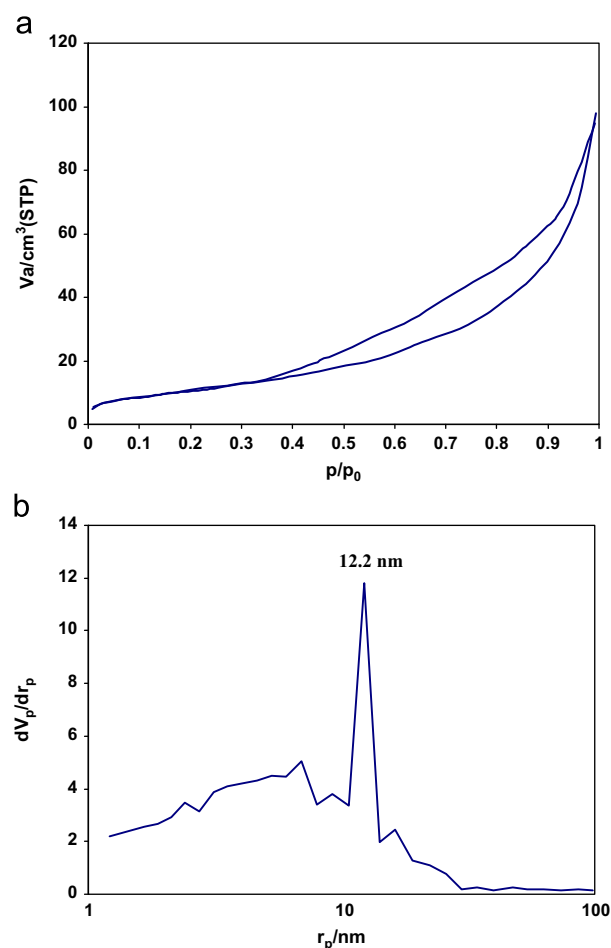


Fig. 4. Nitrogen adsorption–desorption isotherms and (b) the corresponding pore size distribution of the powders calcined at  $900^\circ\text{C}$ .

Table 1  
Textural properties of the powders calcined at 900 °C.

Synthesis method	Specific surface area (m <sup>2</sup> /g)	Mean pore diameter (nm)	Total pore volume(cm <sup>3</sup> /g)
Polyacrylamide gel	34	12	0.13
Conventional sol–gel	14	27	0.06

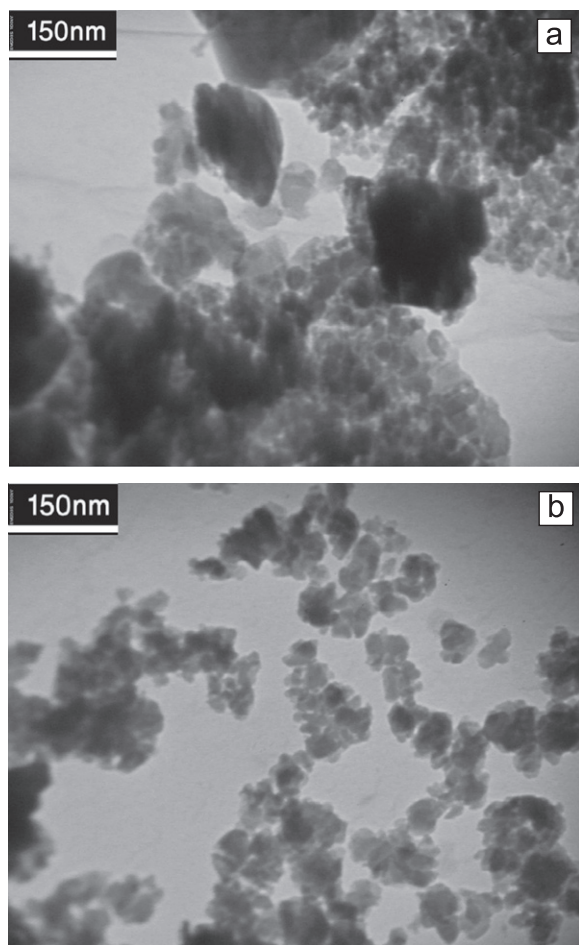


Fig. 5. TEM images of the powders prepared by (a) the conventional sol–gel and (b) polyacrylamide gel methods and heat treated at 900 °C.

where  $S$  is the surface area (m<sup>2</sup> g<sup>−1</sup>),  $D$  is the particle size (nm), and  $\rho$  is the density (g cm<sup>−3</sup>). This equation is based on the assumption that the particles are spherical. The particle diameters calculated from the BET results for the powders prepared by the polyacrylamide gel and conventional sol–gel methods, are about 45 and 130 nm, respectively.

Fig. 5 shows the TEM images of the nanopowders prepared by the conventional sol–gel and polyacrylamide gel methods. Irregular shaped particles were formed by these processes. Larger particles and agglomerates were observed in the powders synthesized via the conventional sol–gel method. In the polyacrylamide gel method, gelation of the solution is achieved by the formation of an organic polymer network. This organic network-cage can cause an increase in the distance between metal cations [22].

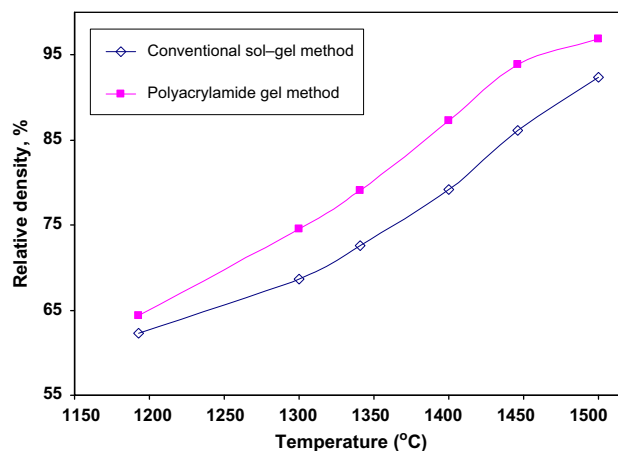


Fig. 6. The relative density of samples prepared as a function of sintering temperature.

Therefore, weaker interactions among primary particles occur during crystallization, leads to a powder with smaller particle sizes and fewer agglomerates. The average particle size of the powders prepared by the polyacrylamide gel method was about 30–80 nm which was relatively in agreement with the BET analysis. The higher surface area of these powders (Table 1) was also attributed to the smaller particle sizes and fewer agglomerates.

Fig. 6 depicts the relative density of samples prepared by the polyacrylamide gel and conventional sol–gel methods as a function of sintering temperature. The relative density was 97% for the samples prepared by the polyacrylamide gel method and sintered at 1500 °C for 3 h, whereas a relative density of 92% was attained for the samples prepared by the conventional sol–gel method under the same sintering conditions. The existence of stronger and larger agglomerates in the samples prepared by the conventional sol–gel method has a negative effect on the increase of density. It was found that dry pressing of nanopowders can cause a green body microstructure with two types of pores. One group is interagglomerate pores which have micrometer scales. These pores coexist with smaller intercrystallite pores (nanometric) within the agglomerate itself [23]. During the sintering, intercrystallite pores shrink and are eliminated, but elimination of the interagglomerate pores requires higher temperatures.

#### 4. Conclusion

A polyacrylamide gel method was used to prepare nanosized europium doped forsterite (Mg<sub>2</sub>SiO<sub>4</sub>:Eu<sup>3+</sup>). An amorphous nanopowder was synthesized. The single-phase forsterite could be formed at a relatively low temperature of about 700 °C without unreacted phases. Average particle size of the powders was about 50 nm. Few agglomerates were observed in the powders. The powders prepared by the polyacrylamide gel method showed better sinterability than the powders synthesized by the conventional sol–gel method.

## Acknowledgments

The work has been financially supported by the Islamic Azad University, Najafabad Branch.

## References

- [1] Hongmei Yang, Jianxin Shi, Menglian Gong, K.W. Cheah, *Journal of Luminescence* 118 (2006) 257.
- [2] Matthew B.D. Mitchell, David Jackson, F. James, *Journal of Sol–Gel Science and Technology* 13 (1998) 359.
- [3] M.T. Tsai, *Materials Research Bulletin* 37 (2002) 2213.
- [4] V. Petricevic, S.K. Gayen, R.R. Alfano, K. Yamagishi, H. Anzai, Y. Yamaguchi, *Applied Physics Letters* 52 (1988) 1040.
- [5] Ganngam Phaomei, W. Rameshwor Singh, R.S. Ningthoujam, *Journal of Luminescence* 131 (2011) 1164.
- [6] Feng Zhang, Yuhua Wang, Yan Wen, Dan Wang, Ye Tao, *Optical Materials* 33 (2011) 475.
- [7] H. Shabir, B. Lal, M. Rafat, *Journal of Sol–Gel Science and Technology* 53 (2010) 399.
- [8] C. Kosanovic, N. Stubicar, N. Tomasic, V. Bermanec, M. Stubicar, *Journal of Alloys and Compounds* 389 (2005) 306.
- [9] S.J. Kiss, E. Kostic, D. Djurovic, S. Bošković, *Powder Technology* 114 (2001) 84.
- [10] A. Kazakos, S. Komarneni, R. Roy, *Materials Letters* 9 (1990) 405.
- [11] J.M. Burlitch, M.L. Beeman, B. Riley, D.L. Kohlstedt, *Chemistry of Materials* 3 (1991) 692.
- [12] K.P. Sanosh, A. Balakrishnan, L. Francis, T.N. Kim, *Journal of Alloys and Compounds* 495 (2010) 113.
- [13] H. Zhang, X. Fu, S. Niu, G. Sun, Q. Xin, *Journal of Solid State Chemistry* 177 (2004) 2649.
- [14] A.K. Adak, S.K. Saha, P. Pramanik, *Journal of Materials Science Letters* 16 (1997) 234.
- [15] S.A. Hassanzadeh-Tabrizi, E. Taheri-Nassaj, H. Sarpoolaky, *Journal of Alloys and Compounds* 456 (2008) 282.
- [16] D. Boyer, G. Bertrand-Chadeyron, R. Mahiou, C. Caperaa, J.C. Cousseins, *Journal of Materials Chemistry* 9 (1998) 211.
- [17] M.T. Tsai, *Journal of Non-Crystalline Solids* 298 (2002) 116.
- [18] S.Q. Wu, Y.Y. Liu, L.N. He, F.P. Wang, *Materials Letters* 58 (2004) 2772.
- [19] K.S.W. Sing, D.H. Everett, R.A.W. Haul, L. Moscou, R.A. Pierotti, J. Rouquerol, T. Siemieniewska, *Pure and Applied Chemistry* 57 (1985) 603.
- [20] X. Liu, J. Yang, L. Wang, X. Yang, L. Lu, X. Wang, *Materials Science and Engineering A* 289 (2000) 241.
- [21] M.B.D. Mitchell, D. Jackson, P.F. James, *Journal of Non-Crystalline Solids* 225 (1998) 125.
- [22] P. Saravanan, M. Padmanabha Raju, S. Alam, *Materials Chemistry and Physics* 103 (2007) 278.
- [23] P. Bowen, C. Carry, *Powder Technology* 128 (2002) 248–255.